# A STANDARD WAVEGUIDE SPARK GAP

David Dettinger and
Robert D. Wengenroth
Wheeler Laboratories, Inc.
Great Neck, N.Y.

Accurately rating the power handling capacity of a microwave component is a frequent and difficult task. In a study of this problem for the Bureau of Ships, a simple waveguide spark gap has been found to be a valuable tool and its adoption by microwave engineers as a universal standard is recommended.

This spark gap has been used to study the effect on breakdown of pulse duration, shape and repetition frequency, of air pressure and motion, of irradiation, and of surface conditions. By measuring the effect on the power required for breakdown as each parameter was varied, it was possible to check the rules for translating data from one set of conditions to another set of conditions.

This spark gap is also useful in routine testing. A regular check, made before the start of a series of tests, will reveal changes in the test apparatus which otherwise might not have been noticed, such as changes in pulse shape or output spectrum. When operation is required at conditions very different from those for which data are available, tests of the spark gap under both sets of conditions will yield the information required to compute the new breakdown level.

## Types of Spark Gap.

A spark gap which is suitable for breakdown testing must satisfy a number of requirements for operation and convenience. These requirements are:

1. Breakdown should occur at an attainable pulse-power level.
2. The unit should appear matched until breakdown occurs.
3. The breakdown level and match should be the same for units built within reasonable machine-shop tolerances.
4. The location of the arc should be known.
5. The surfaces to which the arc strikes should be available for inspection without destroying the gap.
6. Any tuning adjustments should be made without requiring careful electrical or mechanical measurements.
7. The power for breakdown should be computable, at least to a fair approximation.
8. Similarity to typical structures encountered in microwave transmission systems is desirable.
9. Small size is desirable.
10. Low cost of construction is desirable.

Four types of spark gap have been considered for this purpose. They are the resonant section, Fig. 1(a), the swayback guide, Fig. 1(b), the cylindric bump, Fig. 1(c), and the hemispheric bump, Fig. 1(d). (Refs. 2,3). The four types of spark gap may be evaluated by referring to Table 1. Each has advantages and disadvantages as follows:

The resonant-section spark gap is useful for obtaining breakdown with low power but has several disadvantages. It must be sharply tuned. Since the power required for breakdown is dependent upon the spark gap Q, and the Q depends upon the dimensions of the irises at the section ends, the dimensional tolerances for reproducible units are impractically small. The unit is not typical of a transmission system, since the standing waves set up are much higher than those encountered in any typical transmission system. For these reasons the resonant-section spark gap was rejected.

The swayback-guide spark gap is useful where computability is important. By sufficiently decreasing the height of the guide, breakdown may be obtained with much reduced power. This requires close tolerances on the height of the guide if several units are to behave consistently alike. The greatest disadvantage in a swayback-guide spark gap is its length. To obtain good match, the tapers to and from the low-height section must be many wavelengths long. The location of the spark is uncertain and the sparking surface cannot be inspected without removing a wide face. For these reasons, the swayback waveguide was rejected.

The cylindric-bump spark gap is convenient to handle because of its small size, easy to adjust for match by placing two bumps 3/4 wave length apart, typical of capacitive bumps in waveguides, and easy to construct. While it has many of the advantages listed below for the hemispheric bump, the cylindric-bump spark gap requires more power for breakdown and is not so convenient to inspect; for these reasons it was not adopted.

The hemispheric-bump spark gap has all the advantages of the cylindric-bump spark gap, and is computed to break down at one-ninth the normal waveguide breakdown power. The tolerances are typical of those met in waveguide assemblies, and affect mainly the match of the unit. So long as the hemispheric bump is a hemisphere and is small compared to the guide height, its radius does not affect the maximum gradient. The spark location is known; it will occur at one bump. The bump surface may easily be inspected by removing the bump. The bump can be replaced if its surface is damaged. Spacers can be used to adjust the distance between a pair of bumps to approximately 3/4 wavelength to cancel the reflection. The cancellation is noncritical, so only a few spacers are needed to cover the frequency band of a waveguide. The hemisphere is typical of a capacitive bump. The entire unit is small enough to be put into a waveguide system easily. Since the unit is fabricated from waveguide sections and turned hemispheres, it is easy to make. Except where lower breakdown power or a more exact computation of breakdown power reduction is required, this spark gap is satisfactory. Since it meets the requirements for a standard spark gap, the adoption of the hemispheric-bump spark gap is recommended.

Spark Gap Dimensions.

Dimensions for hemispheric-bump spark gaps are given in Figure 2 and Table II for the most common waveguide sizes. The dimensions are noncritical; a bump radius of about one quarter waveguide height is satisfactory and a five percent tolerance on spacing is permissible. The break-

down power level is computed; all dimensions are from the following equations:

Bump radius $r = \frac{b}{4}$

Bump spacing $x = .73\ \lambda_g$

Breakdown peak power $P = .40\ ab\ \frac{\lambda_o}{\lambda_g}$ (in megawatts when a and b are in inches)

The breakdown rating is a computed CW value based on the following assumptions:

1. Peak gradient for breakdown 2.9 Kv/mm in air at atmospheric pressure
2. Gradient tripled on the bump.

Experimental Models.

Hemispheric-bump spark gaps have been built for both X and L-bands. They have been the standard test components for the experimental breakdown measurements made by Wheeler Laboratories. In this service they have performed as expected. Two bumps, spaced approximately 3/4 guide wavelength, were mounted in sections of standard waveguide. Bumps with a radius of about one fourth the guide height were chosen as a compromise between convenience of construction and approximation to the theoretical computation. This size bump is also large compared to the mean free path of an electron in air at pressures encountered in the tests for which this gap is designed; therefore, no allowance need be made for this factor. A hemispheric bump one fourth guide height introduces a reflection of 3 db SWR. For cancellation of reflection the bumps are spaced .73 guide wavelength.

Features built into the experimental models may be seen in Fig. 3. The waveguide walls of the L-band model were reinforced to permit partial evacuation of this unit without danger of the walls collapsing. Since it was to be used in a single narrow band of frequencies, it was built without spacers; therefore, it is fixed tuned. The X-band model was built to cover the 8.5 to 9.6 KMc band; it required spacers, with provisions for sealing against air leaks. Choke flanges were used at each end of each section of the unit; flat plates of the proper thickness having the same face dimensions as cover flanges were used as spacers. A spacer is between the flanges in the photograph. Hose fittings, also visible in the photograph, were installed so that the unit could be mounted between pressure windows with no additional waveguide fittings required for low-pressure tests. These two units illustrate two types of construction for different types of service: a fixed-tuned, narrow-band unit and a tunable, general-purpose unit.

The reduction of power capacity of this type of spark gap below that for uniform waveguide can be computed from the increase in gradient at

the surface of the bump. The gradient is multiplied by a factor of three (see the appendix); therefore, the power for breakdown is one-ninth that of uniform waveguide. The continuous-wave, computed breakdown power for RG-51/U waveguide is about 1.7 Mw in the X-band at atmospheric pressure; therefore, the spark gap should break down at about .19 Mw under these same conditions. Similarly, the L-band gap should break down near 6 Mw.

The hemispheric-bump spark gaps have been used in a number of pulse-power breakdown tests. Typical results are shown in Fig. 4. The procedure for obtaining these data was as follows:

1. The pulse duration, repetition rate, and power level were set to the values desired.
2. Radioactive cobalt was placed so that its radiation penetrated into the volume above one hemisphere.
3. The pressure was reduced slowly until breakdown occurred.

Two degrees of breakdown were noted. As pressure was reduced, groups of pulses would breakdown intermittently. This was called "spitting". Further reduction in pressure resulted in a continuous discharge, which was called an "arc". No sharp line of distinction exists; the data are therefore somewhat uncertain.

Fig. 4 is a plot of points taken by reducing the pressure with the peak power in the pulses constant, but with the repetition frequency varied. The data, extrapolated from low pressure by the law of power-proportional-to-pressure-squared, are plotted against the off-time. Off-time is the actual parameter which is important, since it is during this period that cleanup of the ions occurs. Any ions left at the end of the off-time are available to start a rapid buildup during the next pulse and thus to affect the breakdown level.

Conclusions.

The hemisphere type of spark gap has many advantages over other types. It breaks down at about one-ninth the power capacity of the waveguide, as indicated by an approximate computation based on its simple geometric properties. It is well matched over a moderate bandwidth. Its structure insures that the arc will occur at a known location, which can readily be irradiated. In addition, it is small in size, convenient to inspect, easy to reproduce and inexpensive to fabricate for any waveguide size.

As a comparison standard of power capacity the spark gap is expected to prove preferable to straight waveguide. The latter is simple in concept, but extremely difficult to measure in practice. Most magnetrons available today deliver power well below waveguide capacity; as a matter of practical experience, they are marginally capable of breaking down the hemisphere type of spark gap at atmospheric pressure. Furthermore, since the power capacity of a waveguide run is usually limited by some component having only a fraction of the power capacity of straight waveguide, it is desirable to use a standard comparable to such components in power capacity.

Rating components relative to a spark gap would commonly simplify the entire design procedure by providing the engineer with realistic ratings.

If such a spark gap were universally used, it would serve as a common denominator in correlating measurements made on different test facilities, as well as checking the day-to-day operation of each. It is our recommendation that a waveguide spark gap of the hemisphere type be adopted for standard use with all microwave breakdown test facilities.

## Appendix -- Theoretical Derivation

The computation of the power required for breakdown at the hemispheric-bump spark gap requires a knowledge of the increase in gradient resulting from the insertion of the bump into the waveguide section. An approximate solution will be given for the case where the bump radius is a small fraction of the waveguide height.

An exact computation of the increase in voltage gradient caused by the hemispheric-bump, be setting up and solving the electromagnetic equations for the region, is very difficult because of the geometry of the problem. An analogous problem in electrostatics, however, can be solved with comparative ease.

Harnwell (Ref. 1) demonstrates that a pair of charges, +q and -qr/s located as shown in Fig. 5(a) set up the spherical zero-potential surface of radius "r". Superposing an additional pair of charges of opposite polarity and opposite, collinear position, as in Fig. 5(b), will result in the system shown; the spherical zero-potential surface remains and an additional zero-potential plane is set up by the symmetry of the charges. In addition, when the distance "s" is great, as is now assumed, the equipotential surfaces will approach plane surfaces in a region between the spherical surface and the outer charge. This is indicated on the figure. In the case where the two charges +qr/s and -qr/s are absent, equipotential surfaces will be planes throughout the central region. The central, zero-potential surface may be considered as representing one wall of the waveguide; the spherical surface represents the hemispheric bump; another equipotential, which is a plane because of its distance from the center pair of charges represents the opposite wall of the waveguide. From this electrostatic approximation of the spark gap the increase in gradient at the surface of the bump may be calculated.

The gradient at the surface of the sphere, where the line connecting the charges intersects the sphere, is found by adding the fields set up by the individual charges. For each charge the component of the field is:

$$E = \frac{q}{4\pi e} \frac{1}{d^2} \qquad (1)$$

where

E is the component of the gradient set up by the charge q.

q is the magnitude of the charge being considered.

d is the distance from the charge q to the location of E.

For each charge the gradients at the surface of the bump (A) are as follows (when r is very small compared to s):

$$E = \frac{+q}{4\pi\epsilon}\frac{1}{s^2} \qquad (-q) \qquad (2)$$

$$E = \frac{+q}{4\pi\epsilon}\frac{1}{s^2} \qquad (+q) \qquad (3)$$

$$E = \frac{-q}{4\pi\epsilon}\frac{r}{s}\frac{1}{(r+r^2/s)^2} = \frac{-q}{4\pi\epsilon}\left(\frac{1}{rs} - \frac{2}{s^2}\right) \qquad (+qr/s) \qquad (4)$$

$$E = \frac{+q}{4\pi\epsilon}\frac{r}{s}\frac{1}{(r-r^2/s)^2} = \frac{+q}{4\pi\epsilon}\left(\frac{1}{rs} + \frac{2}{s^2}\right) \qquad (-qr/s) \qquad (5)$$

Without the center pair of charges (no bump):

$$E = \frac{+q}{4\pi\epsilon}\frac{2}{s^2} \qquad (2 + 3) \qquad (6)$$

With the center pair of charges (or with the hemispheric bump):

$$E = \frac{+q}{4\pi\epsilon}\frac{6}{s^2} \qquad (2 + 3 + 4 + 5) \qquad (7)$$

Therefore, the ratio of the gradient on the bump to the gradient on the plane is seen to be 3 to 1.

## References


(1) G.P. Harnwell, "Principles of Electricity and Electromagnetism", 1938. (The method of solving the electrostatic problem of sphere in a field, p. 36).

(2) G.L. Ragan, "Experiments in microwave breakdown", Report 731, Radiation Laboratory, MIT, Nov. 28, 1945. (A report of tests of factors affecting breakdown).

(3) R. Cooper, "Experiments on the electric strength of air at centimeter wavelengths", J.I.E.E., Vol. 94, Part III, pp. 315-324, Sept. 1947. (10.7 cm and 3.06 cm tests).

(4) R.D. Wengenroth, "X-band waveguide spark gap", Wheeler Laboratories Report 494 (Appendix A to third quarterly progress report on Microwave Breakdown Study, Contract No. NObsr 52601), April 1952.

(5) D. Dettinger, "A standard waveguide spark gap", Correspondence section Proc. I.R.E., Vol. 40, p. 1604, Nov. 1952.

COMPARISON OF WAVEGUIDE SPARK GAPS.

| Type of spark gap | Resonant-section | Swayback-guide | Cylindric-bump | Hemispheric-bump |
|---|---|---|---|---|
| Figure | 1(a) | 1(b) | 1(c) | 1(d) |
| Breakdown power relative to guide | Proportional to 1/Q | Proportional to height | 1/4 | 1/9 |
| Method of matching | Tune | Taper | Two bumps spaced for cancellation | Two bumps spaced for cancellation |
| Maintaining tolerances | May be difficult | May be difficult | Easy | Easy |
| Location of Spark | On wide face | One wide face | On cylinder | On hemisphere |
| Method of inspection | Remove face | Remove wide face | Remove cylinder | Remove hemisphere |
| Method of tuning | Side screw or deformed walls, critical | None required, Non-critical | Fixed spacer, non-critical | Fixed spacer, non-critical |
| Breakdown power reduction | Based on Q measurement | Based on waveguide height | Based on approximate rule | Based on approximate rule (Appendix) |
| Relation to waveguide structure | Space between two irises | Reduction of height | Capacitive bump | Capacitive bump |
| Size | Small | Long | Small | Small |
| Work of construction | Moderate | High | Low | Low |

TABLE I

TABLE II

| Typical Spark Gap Dimensions | | | | |
|---|---|---|---|---|
| Waveguide designation RG ( )/U | Bump radius r (in) | Nominal frequency (KMc) | Bump spacing x (in) | Breakdown peak power P (Mw) |
| 69 | 0.810 | 1.300 | 9.260 | 6.0 |
| 48 | 0.335 | 2.900 | 4.220 | 1.06 |
| 51 | 0.125 | 8.500 | 1.290 | 0.18 |
| 51 | 0.125 | 9.375 | 1.110 | 0.19 |
| 51 | 0.125 | 9.600 | 1.072 | 0.19 |
| 52 | 0.100 | 9.375 | 1.284 | 0.10 |
| 91 | 0.078 | 16.000 | 0.670 | 0.062 |
| 53 | 0.042 | 24.000 | 0.521 | 0.016 |

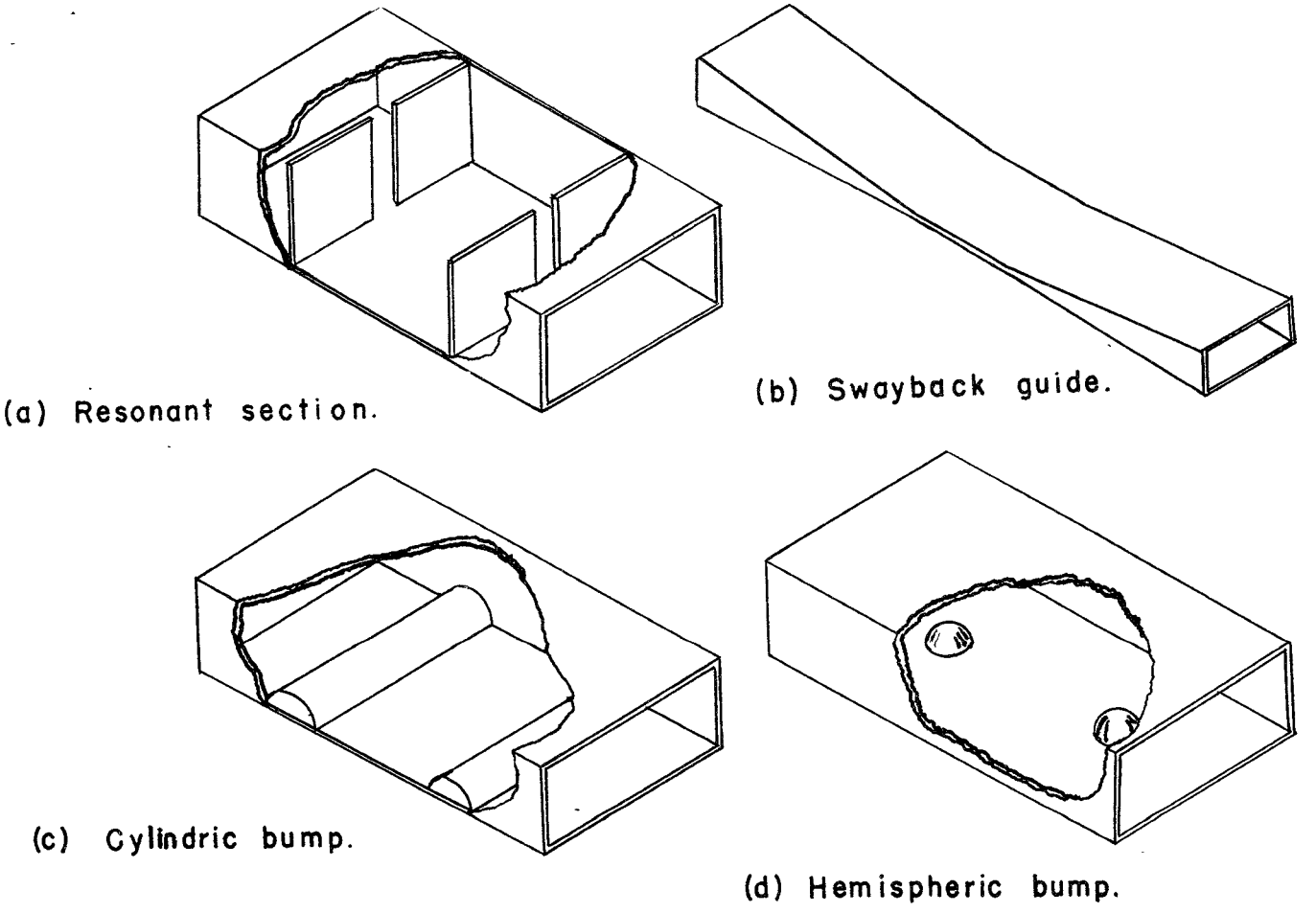


Fig. 1 -- Types of waveguide spark gap.

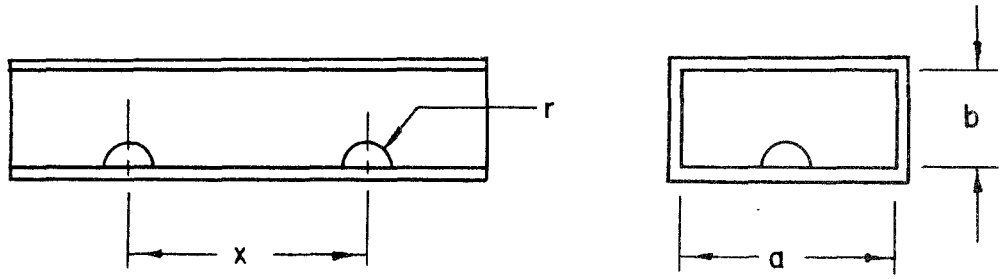


Fig. 2 -- Hemispheric-bump spark gap.

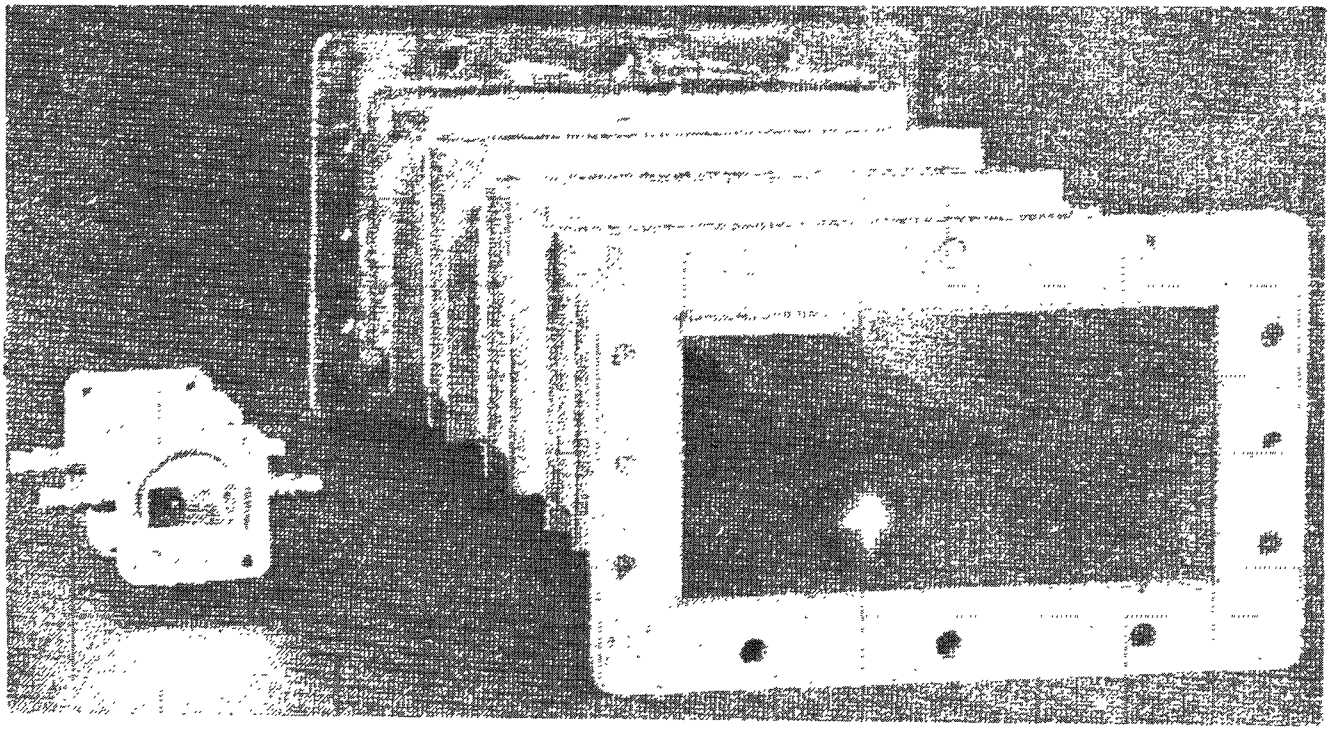

Fig. 3 -- Experimental spark gap.

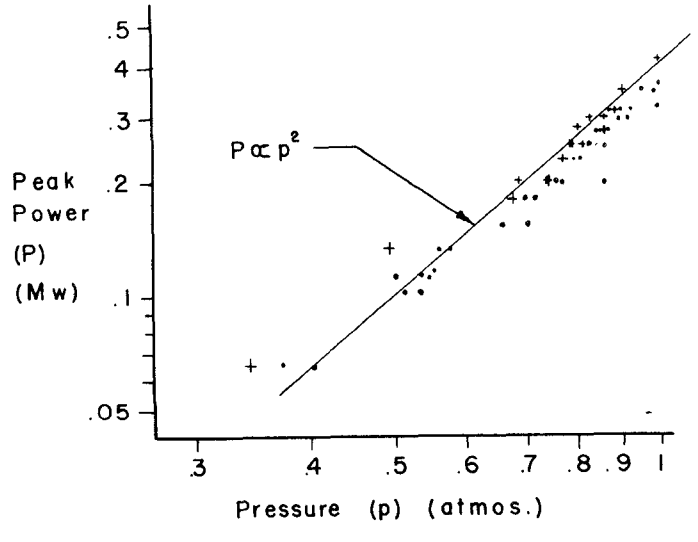


Fig. 4 -- Typical test results.

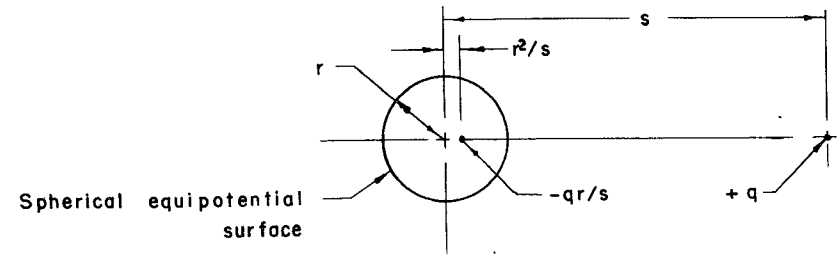


(a) The electrostatic solution for a spherical surface.

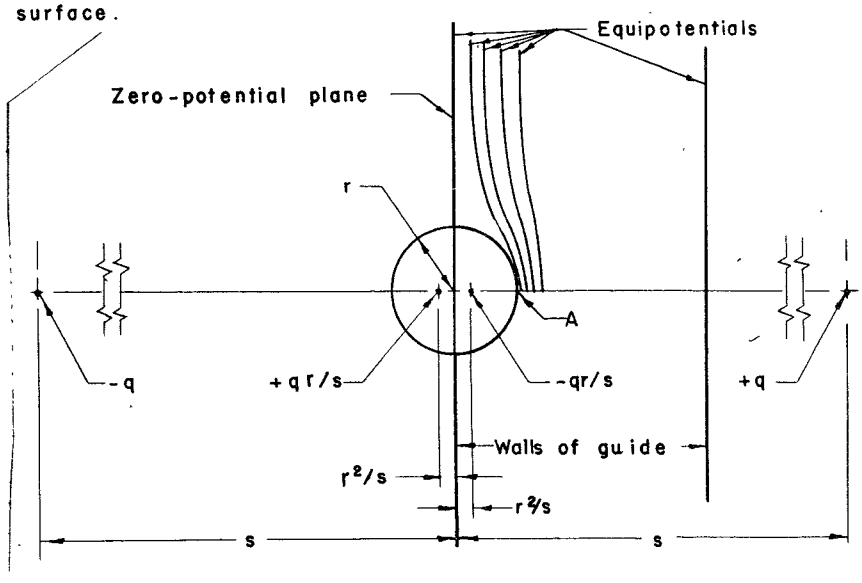


(b) The electrostatic analog to the hemispheric bump.

Fig. 5 -- The electrostatic approximation.

## A ROTARY JOINT FOR TWO MICROWAVE TRANSMISSION CHANNELS OF THE SAME FREQUENCY BAND

Herbert P. Raabe
Wright Air Development Center
Dayton, Ohio.

This dual-channel rotary joint consists of two pairs of rectangular waveguide terminals, a circular waveguide which transmits both channels and coupling elements between the rectangular waveguide terminals and the circular waveguide which convert the rectangular $H_{10}$ mode into the circular $H_{01}$ and $E_{01}$ modes. If pure $H_{01}$ and $E_{01}$ modes can be excited, perfect separation of the channels as well as constant amplitudes and phases can be obtained when the joint rotates. While the conversion into the circular $E_{01}$ mode is performed by a conventional method, a new method had to be developed for the conversion of the rectangular $H_{10}$ mode into the circular $H_{01}$ mode.

(Abstract)